

2023-05-03

# Ultra-Trace Analysis of Fallout Plutonium Isotopes in Soil: Emerging Trends and Future Perspectives

Dowell, SM

<https://pearl.plymouth.ac.uk/handle/10026.1/21422>

---

10.1007/s42250-023-00659-7

Chemistry Africa

Springer Science and Business Media LLC

---

*All content in PEARL is protected by copyright law. Author manuscripts are made available in accordance with publisher policies. Please cite only the published version using the details provided on the item record or document. In the absence of an open licence (e.g. Creative Commons), permissions for further reuse of content should be sought from the publisher or author.*



# Ultra-Trace Analysis of Fallout Plutonium Isotopes in Soil: Emerging Trends and Future Perspectives

Sophia M. Dowell<sup>1,2</sup> · Olivier S. Humphrey<sup>1</sup> · William H. Blake<sup>2</sup> · Odipo Osano<sup>3</sup> · Simon Chenery<sup>1</sup> · Michael J. Watts<sup>1</sup> 

Received: 6 January 2023 / Accepted: 21 March 2023 / Published online: 3 May 2023  
© Crown 2023

## Abstract

The measurement of isotopic abundances and ratio variations of plutonium can provide important information about the sources and behaviours of radiogenic isotopes in the environment. The detection of ultra-trace isotopes of plutonium is increasing interest in the scientific literature for the determination of soil erosion rates due to their long retention times in the environment. The characteristics of plutonium within the environment make it an ideal tracer for the determination of soil redistribution rates and its robustness presents the opportunity to replace more commonly used radioisotopes such as <sup>137</sup>Cesium and <sup>210</sup>Lead. However, ultra-trace analysis of plutonium (fg g<sup>-1</sup>) presents analytical challenges which must be overcome in a variety of soil types. Inductively Coupled Plasma Mass Spectrometry has proven valuable for detection of plutonium in a range of environmental samples. However, severe polyatomic interferences from uranium isotopes significantly limits its application. Due to the improvements in detection sensitivity and reaction cell technology, inductively coupled plasma tandem mass spectrometry, which is also commonly referred to as triple quadrupole inductively coupled plasma tandem mass spectrometry (ICP-MS/MS), has emerged as an exceptional tool for ultra-trace elemental analysis of plutonium isotopes in environmental samples overcoming the limitations of standard quadrupole ICP-MS such as limited sensitivity and cost of analysis. In this review, common methods reported in the literature for the separation and subsequent detection of plutonium isotopes are compared to recent advances in analysis using ICP-MS/MS technology.

---

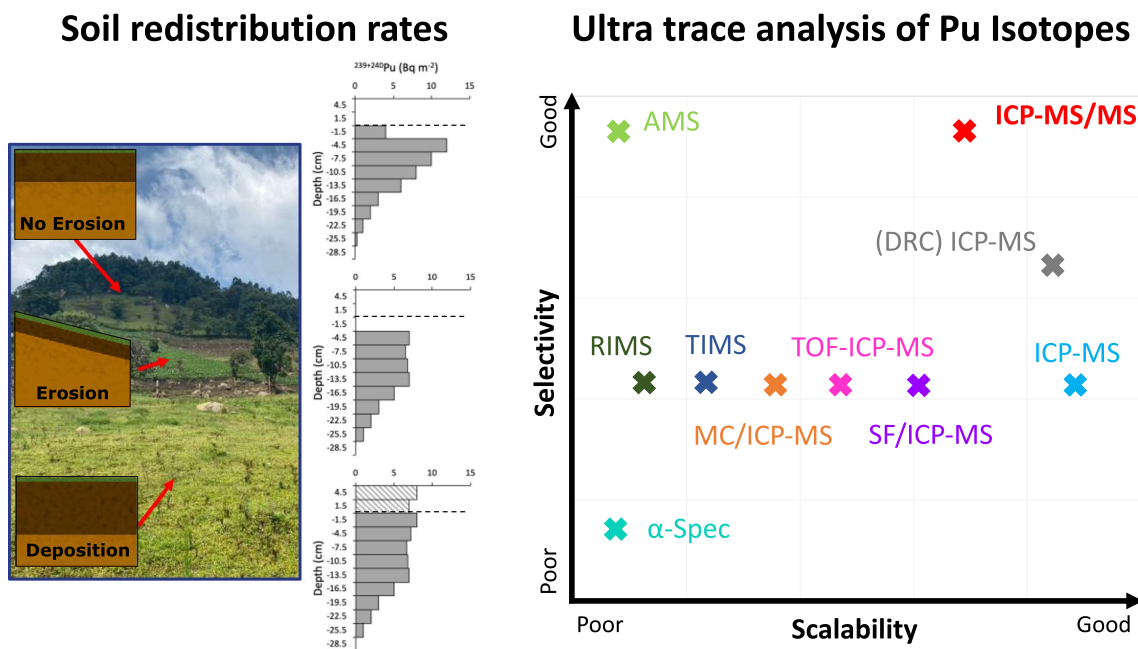
✉ Michael J. Watts  
mwatts@bgs.ac.uk

<sup>1</sup> Inorganic Geochemistry, Centre for Environmental Geochemistry, British Geological Survey, Nottingham NG12 5GG, UK

<sup>2</sup> School of Geography, Earth and Environmental Sciences, University of Plymouth, Plymouth PL4 8AA, Devon, UK

<sup>3</sup> School of Environmental Sciences, University of Eldoret, Eldoret, Kenya

## Graphical Abstract



**Keywords** Plutonium · Soil erosion · Mass spectrometry · Radiometric · ICP-MS/MS

## 1 Introduction

Plutonium (Pu) is an anthropogenic element, ubiquitous in the environment as a result of fallout from nuclear weapons testing in the 1950s and 60s, nuclear power plant accidents and marine discharges of reprocessing waste [1, 2]. However, distribution of Pu from the latter is more localised, owing to  $^{239+240}\text{Pu}$  being contained within the non-volatile fraction of nuclear fuel debris [3, 4]. A total of 520 atmospheric nuclear weapons tests were conducted worldwide between 1945–1980 [5]. Due to their high radiotoxicity and long retention times,  $^{239}\text{Pu}$  and  $^{240}\text{Pu}$  isotopes are considered important transuranic nuclides in the environment with half-lives of 24,110 and 6561 years, respectively [6, 7]. The geographical distribution of Pu in the environment largely varies due to the spatial distribution of weapons testing as well as post-test global weather patterns. The highest deposition is in the northern hemisphere temperate latitudes [8], as only 10% of the overall tests were conducted in the southern hemisphere [9]. This presents a challenge for the analysis of environmental samples in the tropics due to a much lower fallout compared to the mid-latitudes of the northern hemisphere. This can be seen when comparing Europe with Africa, with Europe's minimum activity per unit area being two times larger than Africa's maximum caused by the high

volume of tests in the northern hemisphere in comparison to a much smaller number in the southern hemisphere (Table 1). For the African continent, 14 nuclear weapons tests were conducted within the Tanezrouft region of Algeria, of which only four tests were atmospheric [10, 11].

The analysis of long-lived Pu isotopes are applied as tracers in geochemistry, geochronology, nuclear forensics and as part of environmental monitoring to inform decontamination and remediation strategies [2]. The accurate determination of Pu isotopes could be useful for the identification of contamination sources. For example, global atmospheric fallout has a  $^{240}\text{Pu}/^{239}\text{Pu}$  ratio of 0.18 while much lower ratios (0.02–0.07) are observed via fallout from historical nuclear weapon testing and much higher ratios (0.30–0.41) are observed from releases originating from nuclear power plant accidents and incidents [12–15]. Commonly a sum of both the  $^{239}\text{Pu}$  and  $^{240}\text{Pu}$  isotopes is reported due to the historic use of alpha spectroscopy for their detection. Due to the isotopes similar energies of emission, alpha spectroscopy cannot distinguish between the two isotopes [16].

### 1.1 Environmental Analysis

Plutonium isotopes are considered hazardous pollutants in the environment due to their radiological toxicities and long

**Table 1** Geographical distribution of  $^{239+240}\text{Pu}$  inventories [8]

| Continent     | $^{239+240}\text{Pu}$ range (MBq km <sup>-2</sup> ) |
|---------------|---|
| Africa        | 3.33–19.2   |
| South America | 4.44–22.6   |
| Australia     | 6.66–24.8   |
| Asia          | 55.5–70.3   |
| Europe        | 40.7–115  |
| North America | 12.2–148  |

radioactive half-lives, leading to millennial persistence in the environment [4, 5]. Attention has focused on the impact of these radionuclides on the environment and interest in the biogeochemical behaviour of Pu has been increasing, in particular as an environmental tracer to investigate the origin and delivery pathways [17–19]. The concentrations of Pu isotopes ( $^{239+240}\text{Pu}$ ) in environmental samples are normally very low,  $(0.04 - 400) \times 10^{-16} \text{ g m}^{-3}$  in the atmosphere,  $(10 - 9000) \times 10^{-16} \text{ g g}^{-1}$  in soil and sediment, and  $(0.5 - 22) \times 10^{-16} \text{ g L}^{-1}$  in seawater samples [7]. Since the development of atomic energy from 1940's, nuclear facilities have been established all over the world. With the lifetime of a typical nuclear power plant being between 40 and 60 years, a major concern is the decommissioning of facilities to ensure environmental protection and safety [5]. In order to effectively decommission an area, baseline levels of radionuclides from atmospheric fallout must first be determined within the area close to the site. The analysis of isotopes  $^{238}\text{Pu}$ ,  $^{239}\text{Pu}$  and  $^{240}\text{Pu}$  in a variety of samples matrices is essential to plan decommissioning processes for matrices including concrete, graphite, metals, resin, and filters [19, 20]. Appropriate information for radiological and chemical characterisation is an important factor for legacy waste decommissioning [5].

## 1.2 Soil Redistribution Tracer

Fallout radionuclides (FRN) provide an alternative approach to quantify soil erosion, compared to relatively expensive long-term monitoring techniques such as run-off plot testing. Methods using FRN, in contrast to traditional methods, can be performed within a single sampling campaign and can be applied to the calculation of both erosion and deposition rates. Previously FRN tracing has utilised  $^{137}\text{Cs}$  and  $^{210}\text{Pb}$ , however, Pu isotopes offers a new alternative method which can overcome some of the challenges faced when using both  $^{137}\text{Cs}$  and  $^{210}\text{Pb}$  [4, 21]. Recent advancements, in the quantification of soil redistribution rates, have employed Pu isotopes to determine rates of soil erosion using  $^{239+240}\text{Pu}$  inventory as a measure of soil redistribution [17, 22]. Due to  $^{239}\text{Pu}$  and  $^{240}\text{Pu}$ 's much longer half-lives, about 99% of original activity still remains in soils, providing stable and

long term use for application compared to  $^{137}\text{Cs}$  which has a half-life of only 30 years [23, 24]. Approximately 75% of  $^{137}\text{Cs}$  has already decayed away since the peak of bomb testing and in the northern hemisphere the high spatial variability of fallout from nuclear power plant accidents, such as Chernobyl, make use of  $^{137}\text{Cs}$  as redistribution tracer challenging. More than six times as many atoms of  $^{239+240}\text{Pu}$  were originally dispersed in comparison to  $^{137}\text{Cs}$ , but the specific activity of  $^{137}\text{Cs}$  exceeds that of the Pu isotopes; this makes the Pu isotope more amenable to detection by atom counting methods such as ICP-MS whereas for  $^{137}\text{Cs}$  decay counting by radiometric (gamma) spectrometry is more appropriate [3, 18, 25–28].

The use of  $^{239+240}\text{Pu}$  to determine soil erosion has been reported infrequently in the past [29, 30]. However, in 2001 the use of  $^{239+240}\text{Pu}$  as an alternative to  $^{137}\text{Cs}$  was investigated at a study site in Scheyern farm, southern Germany [22]. Subsequently, there has been an increasing interest in utilising  $^{239+240}\text{Pu}$  as a tracer for soil erosion shown by the increasing number of publications using Pu isotopes for determining rates of soil erosion [24, 31, 32] (Table 2). Due to the increased environmental lifetime and low spatial variability of Pu isotopes compared to  $^{137}\text{Cs}$ , there is an increasing potential for Pu isotopes to replace  $^{137}\text{Cs}$  in the tropics as a soil erosion tracer [4]. Therefore, this review aims to critically assess the current trends in analytical methodologies employed for the detection of Pu isotopes with the following objectives, (i) identification of common methods reported for the determination of Pu isotopes in environmental samples, and (ii) comparison of these methods to identify the usefulness in terms of the determination of soil redistribution rates.

## 2 Methods for Plutonium Determination

### 2.1 Radiochemical Separation of Plutonium

The accurate determination of trace Pu isotopes requires a high level of enrichment prior to analysis due to their low abundance in environmental samples, which is reliant on atmospheric fallout. Using specialised separation techniques, the Pu isotopes can be both removed from the matrix and interfering substances, and pre-concentrated to ensure maximum sensitivity is achieved [42]. For analysis by  $\alpha$ -spectrometry the samples require complete separation of Pu from the matrix to both avoid spectroscopic interferences ( $^{241}\text{Am}$  on  $^{238}\text{Pu}$ ) and obtain a thin alpha source for measurement which must not exceed a few micrometres. This is due to the short range of alpha radiation particles resulting in a degradation of the resolution of Pu peaks in the spectrum as distance increases. This review focuses on the separation techniques employed for mass spectrometry techniques and

**Table 2** Application of Pu analysis for the determination of soil redistribution rates

| Analysis method                                       | References             | Location                 | Country                  |
|---|------------------------|--------------------------|--------------------------|
| Alpha spectrometry                                    | Schimmack et al. [22]  | Scheyern farm            | Germany                  |
|   | Schimmack et al. [33]  | Scheyern farm            | Germany                  |
| AMS   | Hoo et al. [31]        | Camberra                 | Australia                |
|   | Lal et al. [24]        | Northern territory       | Australia                |
|   | Lal et al. [32]        | Daly River               | Australia                |
| ICP-MS with a high efficiency ultrasonic nebuliser    | Xu et al. [34]         | Liaodong Bay             | China                    |
|   | Alewell et al. [17]    | The Urseren Valley       | Switzerland              |
|   | Xu et al. [23]         | Liaodong Bay             | China                    |
|   | Zhang et al. [35]      | Liaodong Bay             | China                    |
|   | Zollinger et al. [36]  | Upper Engadine           | Switzerland              |
|   | Meusbürger et al. [37] | Haean catchment          | South Korea              |
|   | Meusbürger et al. [18] | The Urseren Valley       | Switzerland              |
|   | Raab et al. [26]       | Sila Massif upland       | Italy                    |
|   | Calitri et al. [27]    | Uckermark region         | Germany                  |
|   | Musso et al. [38]      | Klausenpass              | Switzerland              |
|   | Wilken et al. [39]     | Various                  | Uganda, Rwanda, DR Congo |
| ICP-MS/MS   | Wilken et al. [40]     | Weichselian glacial belt | Germany                  |
|   | Khodadadi et al. [3]   | Zarivar Lake             | Iran                     |
|   | Zhang et al. [28]      | Loess Plateau, Qingyang  | China                    |
| ICP-MS/MS with a high efficiency ultrasonic nebuliser | Portes et al. [25]     | Wyoming                  | America                  |
|   | Calitri et al. [41]    | Uckermark region         | Germany                  |

a more detailed explanation of separation for radiometric techniques can be found in Qiao et al. [16].

The matrix elements (salt), peak tailing, and hydrides of  $^{238}\text{U}$  and other polyatomic ions are the major interferences in the measurement of Pu isotopes using ICP-MS [7]. The mass concentrations of Pu are normally very low in environmental samples, and so to maximise the number of atoms counted, large starting masses/volumes of sample are used to pre-concentrate the Pu in the final measured sample aliquot sample. When analysing solid samples, Pu first needs to be released from the solid sample matrix into solution prior to chemical separation. The first preparation step for Pu separation is to remove the organic matter in the sample as otherwise the Pu may bind to these and disrupt the chromatography. Organic matter in the solid samples is commonly decomposed by dry ashing in muffle furnaces at 400–700 °C for 2–24 h [43], although it should be noted that many published studies do not give details of the ashing temperature.

Prior to extraction, samples are spiked with a low abundance isotope such as  $^{242}\text{Pu}$  which can be used as a tracer to calculate recovery following chemical separation and to validate the success of the separation by correction for Pu loss during the analytical process [19, 44, 45]. Concentrated nitric acid is often employed for the extraction of Pu from soil but methods using 8 M nitric acid and aqua regia have also been used [23, 42, 46, 47]. An alternative commonly

used, is a lithium metaborate fusion for samples containing refractory species of Pu, such as samples which have been collected from highly contaminated sites of nuclear weapons tests and nuclear accidents. These refractory species are not fully dissolved by acid leaching which could lead to underestimation of analytical results [48, 49]. However, despite fusion methods being most effective for the digestion of soil samples containing Pu, drawbacks of the method include that additional interfering elements and matrices can also be decomposed leading to unreliable recovery and practicality of fusing large volumes of sample [6].

Co-precipitation, solvent extraction, ion exchange chromatography, and extraction chromatography are often applied for separation and purification of Pu in environmental samples, especially for removal of U [7]. Among the methods in recent years, ion exchange and extraction chromatography are becoming the most popular technique. These methods are based on anionic complexes of Pu with  $\text{NO}_3^-$  and  $\text{Cl}^-$  bonding with the organic functional group within the chromatographic resin [7]. These methods are reliant on Pu existing in the correct oxidation state prior to separation. Since both ion exchange chromatography and extraction chromatography rely on Pu to be in the oxidation state Pu(IV),  $\text{NaNO}_2$  is frequently employed as a valence adjuster to convert Pu to the tetravalent state with the nitrite ion playing an important role in Pu aqueous processing. It

is capable of oxidising Pu(III) to Pu(IV) and of reducing Pu(VI) to Pu(IV). Often another reducing agent, such as ferrous ion is also added to increase the rate of the reaction because the Pu(VI) to Pu(IV) reduction by nitrite is slow [16]. An additional step widely reported to increase the rate of reaction, was the conversion of Pu species to Pu(III) using a reducing agent such as  $K_2S_2O_5$  prior to the addition of  $NaNO_2$  [50, 51]. Co-precipitation with reagents such as Ca, Bi or Fe can be used to reduce the effects of matrix elements on Pu in the sample prior to chromatographic separation [48]. This is often useful for analysis of low mass samples (~ 1 g) to preconcentrate Pu, but is not practical for larger mass soils (e.g., > 50 g) owing to the use of additional chemicals and time-consuming steps.

Nygren et al. [52] investigated the separation of Pu from soil and sediment using different chromatographic methods and found that the TEVA resin (Eichrom Technologies) showed the highest yield of Pu. The potential of this method was further realised when incorporated into a full analytical protocol using ICP-MS by Ketterer et al. [53]. With > 80 citations in google scholar, this paper has become pivotal in the literature, with TEVA resins widely adopted as the standard separation method for Pu isotope measurements for the majority of analytical techniques. This can be attributed to relatively low uranium content within the TEVA resin and relatively large differences in the nitric acid dependency factors of  $k'$  ( $k'$  = distribution coefficient between resin and solution) [54]. The TEVA-resin is based on an aliphatic (R = C8 and C10) quaternary ammonium salt as extractant [52]. To maximise decontamination factors of U isotopes multi-step separations can be used with a combination of resins. Examples of this include, Varga et al. [55] where a UTEVA column was used in tandem with a TRU resin, Metzger et al. [56] used a TEVA column in tandem with UTEVA and Puzas et al. [57] using an AG1-x8 followed by a UTEVA column in tandem with TRU. Through the use of these separation techniques, decontamination factors of U isotopes with respect to Pu of up to  $10^7$  have been achieved [7].

## 2.2 Radiometric Method for Measurement of Plutonium

The determination of Pu isotopes in samples can be achieved in two fundamentally different ways either using: (i) decay counting (radiometric techniques) or (ii) atom counting methods (mass spectroscopy techniques). Alpha spectrometry is the most used radiometric technique for the determination of isotopes  $^{238}Pu$ ,  $^{239+240}Pu$ ,  $^{242}Pu$  and  $^{244}Pu$ . However,  $\alpha$ -spectrometry is unable to distinguish between isotopes with similar energy of emission due to the limited energy resolution of alpha detectors (Table 3) [16]. As a result  $^{239+240}Pu$  isotopes are reported as a sum of activities and

**Table 3** Nuclear properties of Pu isotopes [16, 60]. Note all decays also produce gamma emission but their intensities are too low to be used analytically for environmental samples

| Nuclide    | Half-life (yr)     | Decay mode | Specific activity (Bq $g^{-1}$ ) | Energy of emission (MeV) |
|------------|--------------------|------------|----------------------------------|--------------------------|
| $^{238}Pu$ | 87.7               | $\alpha$   | $6.34 \times 10^{11}$            | 5.59                     |
| $^{239}Pu$ | 24,100             | $\alpha$   | $2.30 \times 10^9$               | 5.16                     |
| $^{240}Pu$ | 6561               | $\alpha$   | $8.40 \times 10^9$               | 5.17                     |
| $^{241}Pu$ | 14.3               | $\beta$    | $3.82 \times 10^{12}$            | 20.8* (KeV)              |
| $^{242}Pu$ | $3.73 \times 10^5$ | $\alpha$   | $1.46 \times 10^8$               | 4.85                     |
| $^{244}Pu$ | $8.08 \times 10^7$ | $\alpha$   | $6.71 \times 10^5$               | 4.59                     |

the method is also unable to distinguish between  $^{238}Pu$  and interfering isotope  $^{241}Am$  [58]. In addition,  $\alpha$ -spectrometry detection of long-lived  $^{242}Pu$  and  $^{244}Pu$  isotopes in environmental samples is challenging due to their ultra-trace level concentrations in the environment and their low specific activity [59].

A typical detection limit of  $\alpha$ -spectrometry is in the order  $10^{-4}$  Bq (0.05 pg)  $^{239}Pu$  [16, 48, 58, 61]. The low cost of instrumentation, high selectivity for alpha particles and high sensitivity resulting from a low background signal make this method attractive for the measurement of Pu isotopes in environmental samples [59]. Although  $\alpha$ -spectrometry has these advantages it is a detection technique which requires very long counting times (1–30 days) and due to the short range of alpha radiation particles and increased thickness may result in a degradation of the resolution of Pu peaks in the spectrum [61]. This means that  $\alpha$ -spectrometry detection is not a suitable method for emergency situations where results are required within a short timeframe or large-scale environmental surveys.

The  $^{241}Pu$  isotope has a principal decay mode via a beta emission meaning that traditionally it has been determined directly by liquid scintillation counting (LSC). It can also be measured indirectly by  $\alpha$ -spectrometry to determine the ingrown daughter  $^{241}Am$  activity [20]. Both methods require a pre-concentration and separation step to allow for analysis and long counting times are required to achieve sufficient counts for an acceptable precision. One of the main challenges of the LSC method is the accurate determination of the counting efficiency which can vary between 30–43%, depending on the spectral quench parameter of the external standard and accounting for these low efficiencies is a challenge [62]. Although initial fallout of  $^{241}Pu$  was high, this isotope is not applicable for use as a soil erosion tracer due to its short half-life and limited environmental lifetime [20].



## 2.3 Mass Spectrometry Techniques

### 2.3.1 Accelerator Mass Spectrometry

The mass spectrometry technique traditionally used for  $^{239+240}\text{Pu}$  measurements in environmental samples is Accelerator Mass Spectrometry (AMS). The instrumental effort is much higher for AMS than for  $\alpha$ -spectrometry, but the much increased sensitivity and ability to distinguish between the isotopes  $^{239}\text{Pu}$  and  $^{240}\text{Pu}$  has in the past made AMS an attractive option for Pu analysis and may be viewed as the “gold standard” technique [58]. The main limitation when using the AMS method to analyse Pu isotopes is the poor availability of specialist facilities where beam time must be applied for to access the facilities and the relatively high cost of using these facilities [34]. However, despite these limitations AMS can achieve very high levels of sensitivity and the method stands out with setting detection limits as low as 0.001 mBq for  $^{239}\text{Pu}$  regardless of the matrix components of the sample, which is between 10–100 times better than detection limits achieved using alpha spectrometry [4, 58, 63–66]. This is possible due to the elimination of molecular isobars in the stripping process, which occurs in the terminal of an electrostatic tandem accelerator [65]. Another benefit of this stripping process is that the levels of U purification prior to analysis are lower than other MS techniques, allowing for the simplification of the radiochemical procedures prior to analysis [66].

### 2.3.2 Thermal Ionisation Mass Spectrometry and Resonance Ionisation Mass Spectrometry

In addition to AMS there are also some alternative mass spectroscopy techniques that are highly sensitive for the detection of Pu isotopes including Thermal Ionisation Mass Spectrometry (TIMS) and Resonance Ionisation Mass Spectrometry (RIMS). The TIMS method has a higher sensitivity for  $^{239}\text{Pu}$  and  $^{240}\text{Pu}$  than ICP-MS and interferences due to UH and  $\text{UH}_2$  are less significant. This means that TIMS has become the method of choice for measuring isotope ratios with precision as low as 0.002% [67]. However, TIMS is

limited by the relatively high cost of analytical facilities and the extensive sample preparation prior to analysis to produce a thin filament source, taking days to weeks of dissolution and separation steps [68]. The method used in RIMS, employs tuned laser beams for the selective excitation of the Pu atoms. It is both highly sensitive and selective for the measurement of  $^{239}\text{Pu}$  with detection of  $^{239}\text{Pu}$  activities as low as 100 atoms per sample, equivalent to of 0.1 nBq. This method however, is only available at specialist laboratories worldwide [4].

### 2.3.3 Inductively Coupled Plasma Mass Spectrometry

An alternative to mass spectrometry methods described above is Inductively Coupled Plasma Mass Spectrometry (ICP-MS). This method has grown in popularity over the past 10 years which is shown by the increasing number of publications using the method and it has become a widely used technique for the detection of Pu isotopes due to its high sensitivity, short analytical times, and relatively simple operation. However, the method can be hindered by the formation of interferences due to polyatomic species, formed from matrix elements and plasma gases. These polyatomic interferences require removal as they have the same integer mass-to-charge ratios as the analyte of interest, leading to false detection or overestimation of results [14, 69]. For Pu isotopes, the major interfering ions are a consequence of the presence of  $^{238}\text{U}$  which is ubiquitous in the environment. Uranium hydrides  $^{238}\text{UH}^+$  and  $^{238}\text{UH}_2^+$  cannot be resolved from  $^{239}\text{Pu}^+$  and  $^{240}\text{Pu}^+$  making analysis of these isotopes a challenge [65]. With the concentration of  $^{238}\text{U}$  in environmental samples being up to 6–9 orders of magnitude higher than that of Pu, another issue for the analysis of  $^{239}\text{Pu}$  as a result, in quadrupole ICP-MS is the peak tailing from  $^{238}\text{U}$  [70]. Therefore, low-resolution ICP-MS cannot always reliably determine  $^{239}\text{Pu}$ , relying heavily on the chemical purification steps prior to analysis, which are used to remove U isotopes from the matrix [71]. However, these procedures also bring additional U into the final sample solutions through atmospheric contamination of the glassware, and reagents [72]. There are also other minor polyatomic interferences which need to be taken into consideration such as plasma gas induced Hg and Pb interferences (Table 4).

**Table 4** Polyatomic interferences for Pu isotopes using ICP-MS [6, 46, 73]

| Isotope           | Polyatomic interference   |
|-------------------|---|
| $^{238}\text{Pu}$ | $^{198}\text{Pt}^{40}\text{Ar}^+$ , $^{201}\text{Hg}^{37}\text{Cl}^+$ , $^{198}\text{Hg}^{40}\text{Ar}^+$ , $^{202}\text{Hg}^{36}\text{Ar}^+$ , $^{205}\text{Ti}^{16}\text{O}_2^+\text{H}^+$ , $^{203}\text{Ti}^{35}\text{Cl}^+$ , $^{208}\text{Pb}^{14}\text{N}^{16}\text{O}^+$ , $^{207}\text{Pb}^{14}\text{N}^{16}\text{O}^+\text{H}^+$ , $^{206}\text{Pb}^{16}\text{O}_2^+$   |
| $^{239}\text{Pu}$ | $^{206}\text{Pb}^{33}\text{S}^+$ , $^{207}\text{Pb}^{16}\text{O}_2^+$ , $^{208}\text{Pb}^{31}\text{P}^+$ , $^{205}\text{Ti}^{34}\text{S}^+$ , $^{203}\text{Ti}^{36}\text{Ar}^+$ , $^{202}\text{Hg}^{37}\text{Cl}^+$ , $^{199}\text{Hg}^{40}\text{Ar}^+$ , $^{203}\text{Ti}^{36}\text{Ar}^+$ , $^{204}\text{Pb}^{35}\text{Cl}^+$ , $^{177}\text{Hf}^{14}\text{N}^{16}\text{O}_3^+$ , $^{176}\text{Hf}^{14}\text{N}^{16}\text{O}_3^+\text{H}^+$ , $^{191}\text{Ir}^{16}\text{O}_3^+$ , $^{193}\text{Ir}^{14}\text{N}^{16}\text{O}_2^+$ , $^{198}\text{Pt}^{40}\text{Ar}^+\text{H}^+$ , $^{208}\text{Pb}^{14}\text{N}^{16}\text{O}^+\text{H}^+$ , $^{209}\text{Bi}^{14}\text{N}^{16}\text{O}^+$                        |
| $^{240}\text{Pu}$ | $^{204}\text{Pb}^{36}\text{Ar}^+$ , $^{206}\text{Pb}^{34}\text{S}^+$ , $^{207}\text{Pb}^{33}\text{S}^+$ , $^{208}\text{Pb}^{32}\text{S}^+$ , $^{205}\text{Ti}^{35}\text{Cl}^+$ , $^{203}\text{Ti}^{37}\text{Cl}^+$ , $^{205}\text{Hg}^{35}\text{Cl}^+$ , $^{200}\text{Hg}^{40}\text{Ar}^+$ , $^{208}\text{Pb}^{16}\text{O}_2^+$ , $^{178}\text{Hf}^{14}\text{N}^{16}\text{O}_3^+$ , $^{177}\text{Hf}^{14}\text{N}^{16}\text{O}_3^+\text{H}^+$ , $^{191}\text{Ir}^{16}\text{O}_3^+\text{H}^+$ , $^{193}\text{Ir}^{14}\text{N}^{16}\text{O}_2^+\text{H}^+$ , $^{194}\text{Pt}^{14}\text{N}^{16}\text{O}_2^+$ , $^{207}\text{Pb}^{16}\text{O}_2^+\text{H}^+$ , $^{209}\text{Bi}^{14}\text{N}^{16}\text{O}^+\text{H}^+$ |

### 2.3.4 Dynamic Reaction Cell/Collision Reaction Cell-Inductively Coupled Plasma Mass Spectrometry

Some studies have focused on the use of dynamic reaction cell (DRC) or collision reaction cell (CRC) ICP-MS to eliminate the  $\text{UH}^+$  interference. The different reactivities of Pu and U with specific gases provide a promising way for the spectro-chemical resolution of  $^{238}\text{Pu}^+$  from isobaric  $^{238}\text{U}^+$  and polyatomic interference i.e.  $\text{UH}^+$  in ICP-MS [70]. Through the introduction of He gas it was reported that the sensitivity of Pu isotopes could be enhanced by about three times, however, the signal of UH species is also enhanced, making it an unsuitable gas to use within the reaction cell [7]. Vais et al. [74] found that the  $^{238}\text{UH}^+$  signal interfering with  $^{239}\text{Pu}$  could be reduced by 10 orders of magnitude by using  $\text{NH}_3$  gas while the Pu signal was only reduced slightly [74]. Tanner et al. [75] and Gourgotis et al. [76] investigated the use of  $\text{CO}_2$  gas for the

reduction of interference, finding that the reaction efficiency of  $\text{UH}^+$  was significantly higher than that of  $\text{Pu}^+$ ; ultimately reducing the interference. The different reactivity observed for U and Pu towards  $\text{CO}_2$  gas is linked to the need to promote the ground-state ions to a reactive configuration with the  $\text{Pu}^+$  ion requiring a greater energy to promote the electron during reaction (1.08 eV) compared to  $\text{U}^+$  (0.04 eV) [75, 76].

### 2.3.5 Inductively Coupled Plasma Tandem Mass Spectrometry

An emerging technique for the analysis of Pu isotopes is ICP-MS/MS which is also commonly referred to as triple quadrupole ICP-MS (ICP-QQQ-MS). The method has gained popularity over recent years due to the method's achievable low (Table 5) detection limits and ability to remove interferences using collision cell technology. This advancement in interference removal efficiency has led to more applications in nuclear materials analysis and other complementary radiometric techniques [70]. The additional quadrupole mass filter located in the front of the collision-reaction cell allows the pre-selection of species, which prevents the formation of secondary polyatomic interference and improves the efficiency of the cell chemistry in the collision cell (Fig. 1) [73, 77]. Using a second quadrupole peak tailing will be reduced which in turn has the advantage of improving the mass resolution reducing effects of peak tailing. Ammonia ( $\text{NH}_3$ ), carbon dioxide ( $\text{CO}_2$ ) and oxygen gas ( $\text{O}_2$ ) are among the different reaction gases proposed for the removal of  $\text{UH}^+$  and  $\text{UH}_2^+$  interferences by ICP-MS/MS [6, 7, 78, 79].

The reaction of  $\text{U}^+$  and  $\text{UH}^+$  interferences within the reaction cell of the ICP-MS/MS with  $\text{NH}_3$ , work effectively to mass shift interferences away from the Pu isotopes. This is possible as a result of Pu isotopes not reacting with the gas and therefore remaining at the original  $m/z$  ratio while  $\text{U}^+$  and  $\text{UH}^+$  are shifted to a higher ratio [7].

**Table 5** Method detection limits of  $^{239}\text{Pu}$  and  $^{240}\text{Pu}$  reported in the literature using different gas modes with ICP-MS/MS

| References        | Sample introduction system | Instrument   | Gas mode      | Detection limit (fg $\text{g}^{-1}$ ) |                   |
|-------------------|----------------------------|--------------|---------------|---------------------------------------|-------------------|
|                   |                            |              |               | $^{239}\text{Pu}$                     | $^{240}\text{Pu}$ |
| Xing et al. [42]  | None                       | Agilent 8800 | $\text{NH}_3$ | 0.55                                  | 0.09              |
| Xing et al. [6]   | None                       | Agilent 8800 | $\text{NH}_3$ | 0.55                                  | 0.09              |
| Bu et al. [47]    | APEX- $\Omega$             | Agilent 8900 | $\text{NH}_3$ | 0.30                                  | 0.20              |
| Xu et al. [79]    | APEX- $\Omega$             | Agilent 8900 | $\text{NH}_3$ | 0.16                                  | 0.05              |
| Hou et al. [7]    | None                       | Agilent 8800 | $\text{CO}_2$ | 0.11                                  | 0.07              |
| Zhang et al. [73] | None                       | Agilent 8900 | $\text{O}_2$  | 0.06                                  | 0.06              |

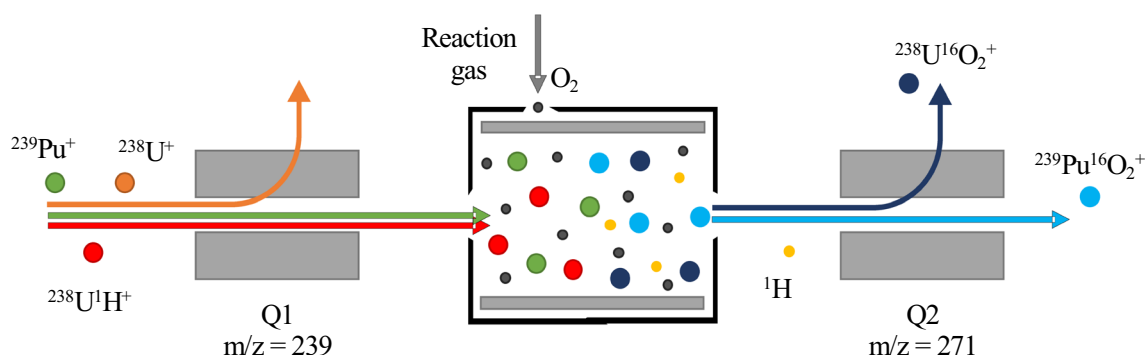
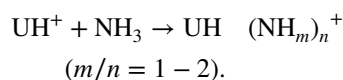
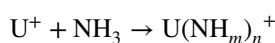


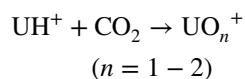
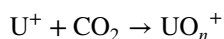
**Fig. 1** Reaction mechanism of  $\text{O}_2$  gas using ICP-MS/MS and  $m/z$  of 239 and 271





Xu et al. [79] reported that both the  $\text{U}^+$  and  $\text{UH}^+$  interferences were effectively eliminated using  $0.4 \text{ mL min}^{-1}$   $\text{NH}_3$  as a reaction gas and  $6.4 \text{ mL min}^{-1}$  He, reducing the overall interference to  $< 2.4 \times 10^{-7}$ . In addition, Pu sensitivity was increased by the collisional focusing effect of He gas to a sensitivity of  $13,900 \text{ Mcps (mg L}^{-1}\text{)}^{-1}$ . Despite the ability of  $\text{NH}_3$  to react with the U interference, the use of  $\text{NH}_3$  gas poses several safety concerns, including its potential corrosive nature, requiring mitigation for its use in a laboratory that could be prohibitively costly [80]. In addition, the ratio of  $\text{UH}^+/\text{U}^+$ , although significantly reduced, is not sufficient to meet the needs of measurement of ultra-low-level Pu in samples containing comparatively higher U concentrations [77].

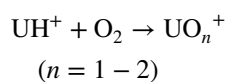
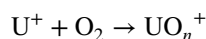
Another commonly used gas is  $\text{CO}_2$  which has been successfully used to eliminate  $\text{UH}^+$  interference by converting hydrides within the sample to oxides, while keeping the intensity of the Pu signal. Both the tailing effect of  $^{238}\text{U}$  on abundance sensitivity and the polyatomic interference  $\text{UH}^+$  are eliminated, reducing the overall interference of uranium to three orders of magnitude better than conventional ICP-MS [7].



Hou et al. [49] reported that the optimal conditions to eliminate U interferences was  $1.2 \text{ mL min}^{-1}$   $\text{CO}_2$  and  $8 \text{ mL min}^{-1}$  He, which reduced overall interference on  $^{239}\text{Pu}$  to  $< 1 \times 10^{-8}$ . However, it was reported that although this high flow rate is optimal for the removal of interfering ions, increasing flow rates above  $1.2 \text{ mL min}^{-1}$  of  $\text{CO}_2$  results in declining intensity of  $\text{PuO}^+$  signal. This was attributed to the increased production of  $\text{PuO}_2^+$  within the collision cell [7]. Similar results were reported by Childs et al. [77] where significant U interferences were observed when comparing a U spiked Pu standard with an un-spiked standard; therefore it was deemed that Pu quantification was not possible using high flow rates of  $\text{CO}_2$  [77]. As the  $m/z$  ratio for  $\text{PuO}_2^+ > 271$  is beyond the mass range for older ICP-MS/MS instruments, the loss of Pu signal measured

at the  $\text{Pu}^+$  mass rather than shifted to an oxide form can have a negative impact on the measurement sensitivity. User requirements, particularly the nuclear industry, for analysing heavy elements in mass shift modes has meant that new instruments such as the Agilent 8900 have an extended  $m/z$  detection range up to 275, allowing for the detection of the mass shifted Pu isotope [73]. This highlights a need for manufacturers to extend the  $m/z$  range in future instruments to improve reaction cell chemistry and therefore allow for greater research into elements with complex interferences, further reducing detection limits and increasing sensitivity.

In addition to  $\text{NH}_3$  and  $\text{CO}_2$ ,  $\text{O}_2$  has also been used as a reaction gas with the  $\text{Pu}^+$  ion readily converted to both  $\text{PuO}^+$  and  $\text{PuO}_2^+$  [73]. Of these two ions the favoured one for analysis is  $\text{PuO}_2^+$  as it is subject to lesser interference than  $\text{PuO}^+$  which experiences dominant interference from uranium oxides,  $^{238}\text{U}^{16}\text{O}^+$ ,  $^{238}\text{U}^{16}\text{O}^1\text{H}^+$  and  $^{238}\text{U}^{16}\text{O}^1\text{H}_2^+$  for the measurement of  $^{239}\text{Pu}^{16}\text{O}^+$  and  $^{240}\text{Pu}^{16}\text{O}^+$  ions, causing a less efficient elimination of the uranium interference [7].



Zhang et al. [28] found that both  $^{238}\text{U}^+$  and  $^{238}\text{U}^1\text{H}^+$  preferably reacted with  $\text{O}_2$  to form  $^{238}\text{U}^{16}\text{O}_2^+$  and therefore the interference was significantly reduced. The optimal conditions in order to observe maximal sensitivity of  $^{242}\text{Pu}^+$  ( $880 \text{ Mcps (mg L}^{-1}\text{)}^{-1}$ ) at  $m/z$  274 ( $\text{PuO}_2^+$ ) was obtained using  $0.09 \text{ mL min}^{-1}$   $\text{O}_2$  as a reaction gas and  $12 \text{ mL min}^{-1}$  He [73]. The  $\text{Pu}^+$  signal decreases exponentially by more than 600 times when using  $\text{O}_2/\text{He}$  gas mode as opposed to He only mode and this can be attributed to the formation of  $\text{PuO}_2^+$  when subjected to relatively high  $\text{O}_2$  levels in the reaction cell. The use of this reaction gas is however limited to detectors with  $m/z$  reaching  $> 271$ . The reaction mechanism for the removal of uranium interferences can be seen in Fig. 1. It should be noted that there may still be some tailing of the  $^{238}\text{U}^{16}\text{O}_2^+$  on to  $^{239}\text{Pu}^{16}\text{O}_2^+$ .

Table 5 summarises the detection limits achieved for ICP-MS/MS analysis using reaction gasses. With older ICP-MS/MS instruments being limited to detect  $m/z$  ratios no greater than  $> 271$  one of the most commonly used reaction gases reported in ICP-MS/MS has been  $\text{NH}_3$ . However, with the need for safe gas handling due to the corrosive nature of  $\text{NH}_3$  and the availability of quadrupole systems capable of  $> 271$  amu, alternative methods are beginning to be favoured. With recent advancements in ICP-MS/MS technology allowing for  $m/z$  ratios  $> 271$  to be detected, oxygen

gas presents an exciting development in the detection of Pu isotopes in the presence of U in samples with detection limits exceeding that of  $\text{NH}_3$  and  $\text{CO}_2$ .

### 2.3.6 Sector Field Inductively Coupled Plasma Mass Spectrometry

Limitations in the mass resolution of quadrupole ICP-MS has led to the development of high-resolution mass spectrometers. Sector field ICP-MS (SF-ICP-MS) which is based on the magnetic field approach and uses double focusing, to improve the mass resolution of ion peaks [81, 82]. This is achieved using an electrostatic analyser (ESA) before or after the magnetic field before passing the sample through an exit slit to filter the isotopes. Consequently, compared to a quadrupole system either an improvement in selectivity in high resolution mode or an improvement in the sensitivity as well as a reduction of the noise level can be achieved in low resolution mode (similar to quadrupole); this results in low achievable detection limits in the  $\text{pg kg}^{-1}$  range [83–85]. Another advantage of SF-ICP-MS over traditional ICP-MS is the ability to measure the signals on flat-topped peaks at lower resolutions. This offers an improvement in the measurement of isotope ratio precision over quadrupole based ICP-MS; however, it is important to note that precision is reduced with increasing resolution due to the deterioration of peak shape and is still poorer than that of MC-ICP-MS, where true simultaneous ratio measurements are made. Similarly to traditional quadrupole ICP-MS, SF-ICP-MS requires a high level of decontamination prior to analysis to remove interferences from  $\text{UH}^+$  as even high resolution mode is insufficient to fully remove this interference [86, 87]. This alongside the relatively higher cost of instrumentation and subsequently less common availability, make SF-ICP-MS a less attractive method for the determination of Pu in soil erosion studies. However, SF-ICP-MS is an more appropriate option in cases where a higher degree of specificity is required (e.g. forensic identification of Pu source using isotope ratios) compared to the requirement for soil erosion studies [83, 88].

### 2.3.7 Multi Collector Inductively Coupled Plasma Mass Spectrometry

Multi-collector ICP-MS (MC-ICP-MS) is based on the simultaneous detection of isotopes, eliminating classical sources of uncertainty from the sequential scanning used in ICP-MS [89]. Typically, MC-ICP-MS instruments will

have up to nine faraday cages making up the detection assembly and newer instruments make use of ion counting systems to improve the abundance selectivity. Therefore, MC-ICP-MS can be used for measuring isotope compositions with both high precision and accuracy, and has the advantage of a high ionisation efficiency in comparison to the TIMS, allowing for a larger theoretical mass range of isotopes to be measured [81]. Similarly, to SF-ICP-MS, this analysis method has a requirement for the removal of  $\text{UH}^+$  via extensive separation prior to analysis and one of the challenges which must be overcome using MC-ICP-MS is the limited ‘practical’ mass range—needing repeat analyses to cover broad mass range, hence longer analysis time compared to ICP-MS/MS, limiting sample throughput. A consequence of this is the need to select an internal standard which falls into the mass range which is usually limited between 10% and 30% [90, 91]. Similarly to the SF-ICP-MS instrumentation, MC-ICP-MS is relatively more expensive than ICP-MS/MS, therefore with less availability and slower sample throughput is not suitable to soil erosion studies which need quick analysis of large quantity of samples.

### 2.3.8 Time of Flight Inductively Coupled Plasma Mass Spectrometry

An alternative analysis method is time of flight ICP-MS (ICP-TOF-MS). This technique pushes a packet of sample ions from the ICP into a ion flight tube, accelerates them and then separates the ions of different mass to charge ratio by their drift time [92]. Counting of the ions proceeds in a temporal succession on a microsecond time scale and because the packet of ions was sampled at the same time from the ICP this method of detection is essentially simultaneous [93]. This gives it an advantage of requiring a low sample volume and quick analysis time. However, prior to analysis a high degree of separation is required, and selectivity is similar to that of traditional quadrupole ICP-MS. Although this method does not offer advantages over ICP-MS/MS in terms of analysis for the purpose of soil erosion measurement, it does have a high potential to be used alongside laser ablation for high resolution analysis of impurities in nuclear fuels, nanomaterials and biological matrices [94–97].

## 3 Discussion

This review summarised the advancements of Pu isotope analysis over the past 20 years, by identifying common methods reported for the determination of Pu isotopes in

environmental samples and comparing these methods for their respective advantages for the measurement of soil redistribution rates. A future challenge which must be addressed is the need for ultra-trace analysis of Pu isotopes in soils, so that Pu can be used as an effective tool for the quantification of soil erosion in areas where global fallout is minimal (tropics). Wilken et al. [39] demonstrated the applicability of using  $^{239+240}\text{Pu}$  in tropical Africa for the determination of soil erosion for study sites along the East African Rift Valley system. Despite lower global fallout in the tropics, a relatively high  $^{239+240}\text{Pu}$  baseline inventory was found at the reference sites. Cultivated sites showed signs of substantial soil erosion and sedimentation that exceeded 40 cm over 55 years. However, half of the slope sites at the cropland site in DR Congo fell below the detection limit of ICP-MS analysis, which makes the drawing of conclusions from data generated by traditional techniques very difficult if not impossible. This challenge could be addressed using ICP-MS/MS, through which the removal of  $\text{UH}^+$  interferences greater selectivity can be achieved (Table 4). The observation of extensive soil erosion, yet inability to determine measurable quantities of Pu emphasised the value of Pu isotopes measured by ICP-MS/MS to study the impact of erosion in tropical Africa where the baseline Pu signal is likely to be relatively much lower than in other global regions. With the advancements of Pu analysis using reaction cell technology, analysis challenges such as limited sensitivity and cost of analysis associated with traditional methods of analysis can be overcome. The improved detection limits using ICP-MS/MS can be seen in Table 6 and the use of Pu isotopes to determine soil redistribution rates in challenging environments (low signal), increasing its viability for use in geochemical surveys associated with soil erosion studies.

Both radiometric and mass spectrometry techniques require extensive and time-consuming sample preparation steps prior to analysis which consist of the digestion of soil samples and radiochemical separation from the matrix elements. Radiometric measurements using both alpha-particle spectrometry and LSC are simple and cost-effective techniques for the determination of  $^{238}\text{Pu}$ ,  $^{239+240}\text{Pu}$  and  $^{241}\text{Pu}$ . However, these methods do not have the ability to detect isotopes  $^{239}\text{Pu}$  and  $^{240}\text{Pu}$  individually. In addition, they require relatively long counting times compared to mass spectrometry methods for accurate quantification of Pu at environmental levels summarised in Table 6. Not all of the papers in Table 6 provided sufficient details to provide an in-depth comparison between methods, with many papers missing crucial details about operating conditions. An ideal format for the comparison of methods and to guide future studies would follow the presentation of experimental details by Kazi et al. [98] and Wang et al. [99]. In contrast, mass spectroscopy techniques can provide shorter analysis times and are highly sensitive with detection limits as low

as  $10^{-3} \text{ mBq g}^{-1}$ . Furthermore, these methods have the capability to provide individual isotopic concentrations of  $^{239}\text{Pu}$  and  $^{240}\text{Pu}$ . However, the availability and cost of some mass spectroscopy techniques is a limiting factor. In some cases depending on the intended purpose of the analysis a combination of both radiometric and mass spectroscopy techniques may be used [16]. Although AMS can be considered the gold standard for ICP-MS analysis, the cost of instrumentation set up (approximately \$4 million for the set-up of each facility) and therefore availability of analytical facilities is a major limiting factor, making this method for the determination of Pu in environmental samples unattractive. Alternative mass spectrometric techniques such as SF-ICP-MS and MC-ICP-MS, have the advantage of increased resolution for the determination of isotopic ratios compared to traditional quadrupole ICP-MS, however, they require a comparable level of decontamination prior to analysis to remove interferences from  $\text{UH}^+$ . This challenge can be overcome using reaction cell technology via developments in recent years of ICP-MS/MS to selectively mass shift interferences during analysis, taking advantage of the high throughput capabilities of this instrumentation over other instruments, enabling its broader application to survey scale studies on soil redistribution rates. Although not reported in the literature at this point in time, exciting developments in the field of analytical chemistry using reaction cell technology paired with high resolution SF-ICP-MS and MC-ICP-MS show promise for the future detection of isotopic ratios. However, for the purpose of soil erosion studies the additional costs associated with the setup of these analysis methods and the surplus ability to determine accurate ratios to the requirement of soil erosion measurement, makes it unlikely these methods will be used for this purpose in the future.

## 4 Conclusion

The development of ICP-MS/MS has opened many novel fields of research involving the analysis of Pu isotopes in soils where ultra-trace detection is required, including as a soil erosion tracer. The developments of reaction cell technology clearly demonstrates that ICP-MS/MS can be a routine tool to support Pu analysis in areas of research such as nuclear decommissioning and soil erosion tracing. The advantages that ICP-MS/MS analysis can offer relative to other instrumentation is the increased rate of analysis and subsequent lower costs per sample, meaning that the method has better availability and can be deployed for survey scale research. However, to improve the detection limits of Pu isotopes, developments in mass spectroscopy measurements using oxygen as the reaction gas are

**Table 6** Comparison of analytical techniques for the determination of Pu activity concentrations

| Detection method | References | Sample introduction technique | Instrument                             | Detection limit (mBq)   | Detection limit (Bq kg <sup>-1</sup> ) | Mass of sample (g)    | Pu recovery (%) | Analysis time (s)                             |
|------------------|------------|-------------------------------|--|-------------------------|--|-----------------------|-----------------|---|
| α-spectrometry   | [58]       |                               | Ortec                                  | 0.40                    |  | 2.5–6                 |                 | 4.0 × 10 <sup>4</sup>                         |
|                  | [98]       |                               | Ortec Spectrum Master 920-8            | 0.20                    |  | 1–10                  | 95.5 ± 4.6      | 7.2 × 10 <sup>3</sup> – 3.6 × 10 <sup>5</sup> |
|                  | [100]      |                               | Alpha Analyst                          |                         | 0.01                                   | 50                    | 87.6            |   |
|                  | [101]      |                               | Canberra                               | 2.95 × 10 <sup>3</sup>  |  |                       |                 | 3.65 × 10 <sup>3</sup>                        |
| LSC              | [48]       |                               | Ortec                                  | 0.31                    |  | 20                    | 84              | 1.73 × 10 <sup>5</sup>                        |
|                  | [102]      |                               | Wallac 1220 Quantulus                  |                         | 0.73                                   | 20                    | 75–80           | 1.44 × 10 <sup>4</sup>                        |
|                  | [103]      |                               | Tri-Carb 3180TR/SL                     |                         | 6 × 10 <sup>-3</sup>                   | 5 × 10 <sup>3</sup>   | 80–95           | 3600  |
|                  | [104]      |                               | PERALS Model 8100AB                    |                         | 6.5 × 10 <sup>3</sup>                  | 2                     | 84 ± 7.2        | 250   |
| AMS              | [64]       |                               | Australian National University         | 4.5 × 10 <sup>-7</sup>  |  |                       |                 |   |
|                  | [105]      |                               | Compact AMS system TANDY at ETH Zurich | 8.74 × 10 <sup>-7</sup> |  |                       |                 | 3600  |
|                  | [106]      |                               | Centro Nacional de Aceleradores        | 0.05                    |  |                       | 60–90           | 30  |
| AMS              | [98]       |                               | Isotracer Laboratory                   | 0.11                    |  | 1–10                  | 95.5 ± 4.6      |   |
| TIMS             | [65]       |                               | CNA                                    |                         | 0.013                                  |                       | 70–88           |   |
|                  | [107]      |                               |  |                         | 5 × 10 <sup>-4</sup>                   | 1–20                  | 75–90           |   |
|                  | [108]      |                               | Triton, Thermo Fisher Scientific       | 1.38 × 10 <sup>-8</sup> |  | 1 × 10 <sup>-12</sup> |                 |   |
| ICP-MS           | [74]       |                               | ELAN DRC II Perkin-Elmer               |                         | 0.16                                   |                       |                 |   |
|                  | [75]       |                               | ELAN DRC II Perkin-Elmer               |                         | 1.38                                   |                       |                 |   |
|                  | [109]      | APEX-Ω                        | ELAN5000                               |                         | 9.2                                    |                       | 70–100          | 660   |
|                  | [110]      | APEX-Ω                        | ELAN-DRCII, PerkinElmer                |                         | 6.67                                   | 10                    | 87–102          |   |
|                  | [51]       |                               | X SeriesII Thermo Fisher Scientific    |                         | 2.76                                   | 1–20                  | 90              |   |
| ICP-MS/MS        | [48]       |                               | Agilent 8800                           | 0.08                    |  | 5                     |                 |   |
|                  | [42]       |                               | Agilent 8800                           |                         | 1.3                                    | 1–20                  | 80–90           |   |
|                  | [5]        |                               | Agilent 8800                           |                         | 0.25                                   |                       | 70–85           | 300   |
|                  | [6]        |                               | Agilent 8800                           |                         | 1.3                                    | 10                    |                 |   |
| ICP-MS/MS        | [70]       | APEX-Ω                        | Agilent 8900                           |                         | 0.69                                   |                       | 80              | 120   |
|                  | [73]       |                               | Agilent 8900                           |                         | 0.14                                   |                       |                 |   |
|                  | [79]       | APEX-Ω                        | Agilent 8900                           |                         | 0.37                                   | 1–2                   |                 |   |
| SF-ICP-MS        | [61]       | Aridus                        | ELEMENT                                |                         | 0.30                                   |                       |                 |   |

**Table 6** (continued)

| Detection method | References | Sample introduction technique | Instrument                          | Detection limit (mBq) | Detection limit (Bq kg <sup>-1</sup> ) | Mass of sample (g) | Pu recovery (%) | Analysis time (s) |
|------------------|------------|-------------------------------|-------------------------------------|-----------------------|--|--------------------|-----------------|-------------------|
|                  | [111]      |                               | Element 1<br>Finnigan-MAT           |                       | 3.91                                   |                    |                 |                   |
|                  | [84]       | APEX-Ω                        | Finnigan<br>Element 2<br>Bremen     |                       | 0.32                                   | 0.03 – 0.5         |                 | 150               |
|                  | [83]       |                               | PlasmaTrace 2<br>Micromass          |                       | 0.018                                  |                    |                 |                   |
|                  | [85]       | APEX-Ω                        | Axiom SC VG<br>Elemental            |                       | 0.23                                   |                    |                 |                   |
|                  | [99]       | APEX-Ω                        | Element XR,<br>Thermo<br>Scientific |                       | 0.015                                  | 1                  | 80              | 130               |
| MC-ICP-MS        | [91]       | MCN 6000<br>CETAC             | IsoProbe<br>Micromass               |                       | 9.2                                    |                    |                 |                   |
|                  | [90]       | APEX-Ω                        | NEPTUNE<br>Thermo<br>Fisher         |                       | 0.046                                  | 2                  |                 |                   |
|                  | [112]      | Aridus II                     | NU Instru-<br>ments                 |                       | 0.023                                  |                    |                 |                   |

necessary in order to detect high end  $m/z$  ratios ( $> 271$ ) to further enhance the selectivity for Pu through removal of polyatomic interferences. Additionally, there is a need to refine the separation process prior to analysis to allow for the effective pre-concentration of ultra-trace Pu. This has the potential to increase Pu's applicability to be used as a soil redistribution tracer in challenging environments, such as tropical Africa, where Pu concentrations will be present in soils at ultra-trace levels. This data has the potential to inform land management practices via the better understanding of the rate of soil losses in the tropics.

**Acknowledgements** This work is published with the permission of the Executive Director, British Geological Survey. This work has originated from research conducted with the financial support of the following funders: BGS-NERC grant NE/R000069/1 entitled 'Geoscience for Sustainable Futures' and BGS Centre for Environmental Geochemistry programmes for financial support, the NERC National Capability International Geoscience programme entitled 'Geoscience to tackle global environmental challenges' (NE/X006255/1). In addition, The Royal Society international collaboration awards 2019 grant ICA/R1/191077 entitled 'Dynamics of environmental geochemistry and health in a lake wide basin', Natural Environment Research Councils ARIES Doctoral Training Partnership (grant number NE/S007334/1) and the British Geological Survey University Funding Initiative (GA/19S/017). Additional support provided from the British Academy Early Career Researchers Writing Skills Workshop (WW21100104). The authors would like to thank Drs' Andrew Marriott for checking of the manuscript.

**Data availability** Not available.

## Declarations

**Conflict of Interest** The authors declare that there is no financial/personal interest or belief that could affect their objectivity.

**Open Access** This article is licensed under a Creative Commons Attribution 4.0 International License, which permits use, sharing, adaptation, distribution and reproduction in any medium or format, as long as you give appropriate credit to the original author(s) and the source, provide a link to the Creative Commons licence, and indicate if changes were made. The images or other third party material in this article are included in the article's Creative Commons licence, unless indicated otherwise in a credit line to the material. If material is not included in the article's Creative Commons licence and your intended use is not permitted by statutory regulation or exceeds the permitted use, you will need to obtain permission directly from the copyright holder. To view a copy of this licence, visit <http://creativecommons.org/licenses/by/4.0/>.

## References

- Hu QH, Weng JQ, Wang JS (2010) Sources of anthropogenic radionuclides in the environment: a review. *J Environ Radioact* 101:426–437. <https://doi.org/10.1016/j.jenvrad.2008.08.004>
- Goldstein SJ, Price AA, Hinrichs KA, Lamont SP, Nunn AJ, Amato RS, Cardon AM, Gurganus DW (2021) High-precision measurement of U-Pu-Np-Am concentrations and isotope ratios in environmental reference materials by mass spectrometry. *J Environ Radioact* 237:106689. <https://doi.org/10.1016/j.jenvrad.2021.106689>
- Khodadadi M, Alewell C, Mirzaei M, Ehssan-Malahat EE, Asadzadeh F, Strauss P, Meusburger K (2021) Deforestation effects on soil erosion rates and soil physicochemical properties in Iran: a case study of using fallout radionuclides in a Chernobyl



- contaminated area. *Soil D* (Preprint). <https://doi.org/10.5194/soil-2021-2>
4. Alewell C, Pitois A, Meusburger K, Ketterer M, Mabit L (2017) 239 + 240Pu from ‘contaminant’ to soil erosion tracer: where do we stand? *Earth-Science Rev* 172:107–123. <https://doi.org/10.1016/j.earscirev.2017.07.009>
  5. Hou X (2019) Radioanalysis of ultra-low level radionuclides for environmental tracer studies and decommissioning of nuclear facilities. *J Radioanal Nucl Chem* 322:1217–1245. <https://doi.org/10.1007/s10967-019-06908-9>
  6. Xing S, Luo M, Yuan N, Liu D, Yang Y, Dai X, Zhang W, Chen N (2021) Accurate determination of plutonium in soil by tandem quadrupole ICP-MS with different sample preparation methods. *Atom Spectrosc* 42:62–70. <https://doi.org/10.46770/AS.2021.011>
  7. Hou X, Zhang W, Wang Y (2019) Determination of femtogram-level plutonium isotopes in environmental and forensic samples with high-level uranium using chemical separation and ICP-MS/MS measurement. *Anal Chem* 91:11553–11561. <https://doi.org/10.1021/acs.analchem.9b01347>
  8. Hardy EP, Krey PW, Volchok HL (1973) Global inventory and distribution of fallout plutonium. *Nature* 241:444–445. <https://doi.org/10.1038/241444a0>
  9. Thakur P, Khaing H, Salminen-Paatero S (2017) Plutonium in the atmosphere: a global perspective. *J Environ Radioact* 175–176:39–51. <https://doi.org/10.1016/j.jenvrad.2017.04.008>
  10. Danesi PR, Moreno J, Makarewicz M, Louvat D (2008) Residual radionuclide concentrations and estimated radiation doses at the former French nuclear weapons test sites in Algeria. *Appl Radiat Isotope* 66:1671–1674. <https://doi.org/10.1016/j.apradiso.2007.08.022>
  11. Právělie R (2014) Nuclear weapons tests and environmental consequences: a global perspective. *Ambio* 43:729–744. <https://doi.org/10.1007/s13280-014-0491-1>
  12. Kelley JM, Bond LA, Beasley TM (1999) Global distribution of Pu isotopes and 237Np. *Sci Total Environ* 237–238:483–500. [https://doi.org/10.1016/s0048-9697\(99\)00160-6](https://doi.org/10.1016/s0048-9697(99)00160-6)
  13. Eriksson M, Lindahl P, Roos P, Dahlgaard H, Holm E (2008) U, Pu, and Am nuclear signatures of the thule hydrogen bomb debris. *Environ Sci Technol* 42:4717–4722. <https://doi.org/10.1021/es800203f>
  14. Muramatsu Y, Rühm W, Yoshida S, Tagami K, Uchida S, Wirth E (2000) Concentrations of 239Pu and 240Pu and their isotopic ratios determined by ICP-MS in soils collected from the Chernobyl 30-km zone. *Environ Sci Technol* 34:2913–2917. <https://doi.org/10.1021/es0008968>
  15. Zheng J, Tagami K, Uchida S (2013) Release of plutonium isotopes into the environment from the Fukushima Daiichi nuclear power plant accident: what is known and what needs to be known. *Environ Sci Technol* 47:9584–9595. <https://doi.org/10.1021/es402212v>
  16. Qiao J, Hou X, Miró M, Roos P (2009) Determination of plutonium isotopes in waters and environmental solids: a review. *Anal Chim Acta* 652:66–84. <https://doi.org/10.1016/j.aca.2009.03.010>
  17. Alewell C, Meusburger K, Juretzko G, Mabit L, Ketterer ME (2014) Suitability of 239+240Pu and 137Cs as tracers for soil erosion assessment in mountain grasslands. *Chemosphere* 103:274–280. <https://doi.org/10.1016/j.chemosphere.2013.12.016>
  18. Meusburger K, Porto P, Mabit L, La Spada C, Arata L, Alewell C (2018) Excess Lead-210 and Plutonium-239+240: two suitable radiogenic soil erosion tracers for mountain grassland sites. *Environ Res* 160:195–202. <https://doi.org/10.1016/j.envres.2017.09.020>
  19. Yang G, Zheng J, Kim E, Zhang S, Seno H, Kowatri M, Aono T, Kurihara O (2021) Rapid analysis of 237Np and Pu isotopes in small volume urine by SF-ICP-MS and ICP-MS/MS. *Anal Chim Acta* 1158:338431. <https://doi.org/10.1016/j.aca.2021.338431>
  20. Thakur P, Ward AL (2018) 241Pu in the environment: insight into the understudied isotope of plutonium. *J Radioanal Nucl Chem* 317:757–778. <https://doi.org/10.1007/s10967-018-5946-6>
  21. Loba A, Waroszewski J, Sykuła K, Kabala C, Egli M (2022) Meteoric 10Be, 137Cs and 239+240Pu as tracers of long- and medium-term soil erosion—a review. *Miner* 12:359. <https://doi.org/10.3390/min12030359>
  22. Schimmack W, Auerswald K, Bunzl K (2001) Can 239+240Pu replace 137Cs as an erosion tracer in agricultural landscapes contaminated with Chernobyl fallout? *J Environ Radioact* 53:41–57. [https://doi.org/10.1016/s0265-931x\(00\)00117-x](https://doi.org/10.1016/s0265-931x(00)00117-x)
  23. Xu Y, Qiao J, Pan S, Hou X, Roos P, Cao L (2015) Plutonium as a tracer for soil erosion assessment in northeast China. *Sci Total Environ* 511:176–185. <https://doi.org/10.1016/j.scitotenv.2014.12.006>
  24. Lal R, Tims SG, Fifield LK, Wasson RJ, Howe D (2013) Applicability of 239Pu as a tracer for soil erosion in the wet-dry tropics of northern Australia. *Nucl Instrum Methods Phys Res B Beam Interact Mater Atoms* 294:577–583. <https://doi.org/10.1016/j.nimb.2012.07.041>
  25. Portes R, Dahms D, Brandova D, Raab G, Christl M, Kuhn P, Ketterer M, Egli M (2018) Evolution of soil erosion rates in alpine soils of the Central Rocky Mountains using fallout Pu and 813C. *Earth Planet Sci Lett* 496:257–269. <https://doi.org/10.1016/j.epsl.2018.06.002>
  26. Raab G, Scarciglia F, Norton K, Dahms D, Brandova D, Portes R, Christl M, Ketterer M, Ruppli A, Egli M (2018) Denudation variability of the Sila Massif upland (Italy) from decades to millennia using 10Be and 239+240Pu. *Land Degrad Dev* 29:3736–3752. <https://doi.org/10.1002/ldr.3120>
  27. Calitri F, Sommer M, Norton K, Temme A, Brandova D, Portes R, Christl M, Ketterer M, Egli M (2019) Tracing the temporal evolution of soil redistribution rates in an agricultural landscape using 239+240Pu and 10Be. *Earth Surf Process Landforms* 44:1783–1798. <https://doi.org/10.1002/esp.4612>
  28. Zhang W, Xing S, Hou X (2019) Evaluation of soil erosion and ecological rehabilitation in Loess Plateau region in Northwest China using plutonium isotopes. *Soil Tillage Res* 191:162–170. <https://doi.org/10.1016/j.still.2019.04.004>
  29. Muller RN, Sprugel DG, Kohn B (1978) Erosional transport and deposition of plutonium and cesium in two small midwestern watersheds. *J Environ Qual* 7:171–174. <https://doi.org/10.2134/jeq1978.00472425000700020003x>
  30. Joshi SR, Shukla BS (1991) AB initio derivation of formulations for 210Pb dating of sediments. *J Radioanal Nucl Chem* 148:73–79. <https://doi.org/10.1007/BF02060548>
  31. Hoo WT, Fifield LK, Tims SG, Fujioka T, Mueller N (2011) Using fallout plutonium as a probe for erosion assessment. *J Environ Radioact* 102:937–942. <https://doi.org/10.1016/j.jenvrad.2010.06.010>
  32. Lal R, Fifield LK, Tims SG, Wasson RJ, Howe D (2020) A study of soil erosion rates using 239Pu, in the wet-dry tropics of northern Australia. *J Environ Radioact* 211:106085. <https://doi.org/10.1016/j.jenvrad.2019.106085>
  33. Schimmack W, Auerswald K, Bunzl K (2002) Estimation of soil erosion and deposition rates at an agricultural site in Bavaria, Germany, as derived from fallout radiocesium and plutonium as tracers. *Naturwissenschaften* 89:43–46. <https://doi.org/10.1007/s00114-001-0281-z>
  34. Xu Y, Qiao J, Hou X, Pan S (2013) Plutonium in soils from northeast China and its potential application for evaluation of soil erosion. *Sci Rep* 3:1–8. <https://doi.org/10.1038/srep03506>



35. Zhang K, Pan S, Xu Y, Cao L, Hao Y, Wu M, Xu W, Ren S (2016) Using  $^{239+240}\text{Pu}$  atmospheric deposition and a simplified mass balance model to re-estimate the soil erosion rate: a case study of Liaodong Bay in China. *J Radioanal Nucl Chem* 307:599–604. <https://doi.org/10.1007/s10967-015-4208-0>
36. Zollinger B, Alewell C, Kneisel C, Meusbürger K, Brandová D, Kubik P, Schaller M, Ketterer M, Egli M (2015) The effect of permafrost on time-split soil erosion using radionuclides ( $^{137}\text{Cs}$ ,  $^{239+240}\text{Pu}$ , meteoric  $^{10}\text{Be}$ ) and stable isotopes ( $\delta^{13}\text{C}$ ) in the eastern Swiss Alps. *J Soils Sediments* 15:1400–1419. <https://doi.org/10.1007/s11368-014-0881-9>
37. Meusbürger K, Mabit L, Ketterer M, Park J, Sandor T, Porto P, Alewell C (2016) A multi-radionuclide approach to evaluate the suitability of  $^{239+240}\text{Pu}$  as soil erosion tracer. *Sci Total Environ* 566:1489–1499. <https://doi.org/10.1016/j.scitotenv.2016.06.035>
38. Musso A, Ketterer M, Greinwald K, Geitner C, Egli M (2020) Rapid decrease of soil erosion rates with soil formation and vegetation development in periglacial areas. *Earth Surf. Process. Landforms* 45:2824–2839. <https://doi.org/10.1002/esp.4932>
39. Wilken F, Fiener P, Ketterer M, Meusbürger K, Muhindo DL, van Oost K, Doetterl S (2021) Assessing soil erosion of forest and cropland sites in wet tropical Africa using  $^{239+240}\text{Pu}$  fallout radionuclides. *Soil* 7:399–414. <https://doi.org/10.5194/soil-7-399-2021>
40. Wilken F, Ketterer M, Koszinski S, Sommer M, Fiener P (2020) Understanding the role of water and tillage erosion from  $^{239+240}\text{Pu}$  tracer measurements using inverse modelling. *SOIL* 6:549–564. <https://doi.org/10.5194/soil-6-549-2020>
41. Calitri F, Sommer M, van der Meij MW, Egli M (2020) Soil erosion along a transect in a forested catchment: Recent or ancient processes? *CATENA* 194:104683. <https://doi.org/10.1016/j.catena.2020.104683>
42. Xing S, Zhang W, Qiao J, Hou X (2018) Determination of ultra-low level plutonium isotopes ( $^{239}\text{Pu}$ ,  $^{240}\text{Pu}$ ) in environmental samples with high uranium. *Talanta* 187:357–364. <https://doi.org/10.1016/j.talanta.2018.05.051>
43. Wang Z, Yang G, Zheng J, Cao L, Yu H, Zhu Z, Tagami K, Uchida S (2015) Effect of ashing temperature on accurate determination of plutonium in soil samples. *Anal Chem* 87:5511–5515. <https://doi.org/10.1021/acs.analchem.5b01472>
44. Jerome SM, Smith D, Woods MJ, Woods SA (1995) Metrology of plutonium for environmental measurements. *Appl Radiat Isot* 46:1145–1150. [https://doi.org/10.1016/0969-8043\(95\)00157-9](https://doi.org/10.1016/0969-8043(95)00157-9)
45. Gao RQ, Hou XL, Zhang LY, Zhang WC, Zhang MT (2020) Determination of ultra-low level plutonium isotopes in large volume environmental water samples. *Chin J Anal Chem* 48:765–773. [https://doi.org/10.1016/S1872-2040\(20\)60027-5](https://doi.org/10.1016/S1872-2040(20)60027-5)
46. Wang Z, Zheng J, Ni Y, Men W, Tagami K, Uchida S (2017) High-performance method for determination of Pu isotopes in soil and sediment samples by sector field-inductively coupled plasma mass spectrometry. *Anal Chem* 89:2221–2226. <https://doi.org/10.1021/acs.analchem.6b04975>
47. Bu W, Zheng J, Guo Q, Aono T, Otosaka S, Tagami K, Uchida S (2015) Temporal distribution of plutonium isotopes in marine sediments off Fukushima after the Fukushima Dai-ichi Nuclear Power Plant accident. *J Radioanal Nucl Chem* 303:1151–1154. <https://doi.org/10.1007/s10967-014-3437-y>
48. Luo M, Xing S, Yang Y, Song L, Ma Y, Wang Y, Dai X, Happel S (2018) Sequential analyses of actinides in large-size soil and sediment samples with total sample dissolution. *J Environ Radioact* 187:73–80. <https://doi.org/10.1016/j.jenvrad.2018.01.028>
49. Maxwell SL, Culligan B, Hutchison JB, McAlister DR (2015) Rapid fusion method for the determination of Pu, Np, and Am in large soil samples. *J Radioanal Nucl Chem* 305:599–608. <https://doi.org/10.1007/s10967-015-3992-x>
50. Cao L, Bu W, Zheng J, Pan S, Wang Z, Uchida S (2016) Plutonium determination in seawater by inductively coupled plasma mass spectrometry: a review. *Talanta* 151:30–41. <https://doi.org/10.1016/j.talanta.2016.01.010>
51. Qiao J, Hou X, Roos P, Miró M (2010) Rapid and simultaneous determination of neptunium and plutonium isotopes in environmental samples by extraction chromatography using sequential injection analysis and ICP-MS. *J Anal Atom Spectrom* 25:1769–1779. <https://doi.org/10.1039/C003222K>
52. Nygren U, Rodushkin I, Nilsson C, Baxter DC (2003) Separation of plutonium from soil and sediment prior to determination by inductively coupled plasma mass spectrometry. *J Anal Atom Spectrom* 18:1426–1434. <https://doi.org/10.1039/B306357G>
53. Ketterer ME, Hafer KM, Jones VJ, Appleby PG (2004) Rapid dating of recent sediments in Loch Ness: inductively coupled plasma mass spectrometric measurements of global fallout plutonium. *Sci Total Environ* 322:221–229. <https://doi.org/10.1016/j.scitotenv.2003.09.016>
54. Horwitz EP, Dietz ML, Chiarizia R, Diamond H, Maxwell SL, Nelson MR (1995) Separation and preconcentration of actinides by extraction chromatography using a supported liquid anion exchanger: application to the characterization of high-level nuclear waste solutions. *Anal Chim Acta* 310:63–78. [https://doi.org/10.1016/0003-2670\(95\)00144-0](https://doi.org/10.1016/0003-2670(95)00144-0)
55. Varga Z, Surányi G, Vajda N, Stefánka Z (2007) Determination of plutonium and americium in environmental samples by inductively coupled plasma sector field mass spectrometry and alpha spectrometry. *Microchem J* 85:39–45. <https://doi.org/10.1016/j.microc.2006.02.006>
56. Metzger SC, Rogers KT, Bostock DA, McBay EH, Ticknor BW, Manard BT, Hexel CR (2019) Optimization of uranium and plutonium separations using TEVA and UTEVA cartridges for MC-ICP-MS analysis of environmental swipe samples. *Talanta* 198:257–262. <https://doi.org/10.1016/j.talanta.2019.02.034>
57. Puzas A, Genys P, Remeikis V, Druteikienė R (2014) Challenges in preparing soil samples and performing a reliable plutonium isotopic analysis by ICP-MS. *J Radioanal Nucl Chem* 303:751–759. <https://doi.org/10.1007/s10967-014-3411-8>
58. Hrncsek E, Steier P, Wallner A (2005) Determination of plutonium in isotopic samples by AMS and alpha spectrometry. *Appl Radiat Isotope* 63:633–638. <https://doi.org/10.1016/j.apradiso.2005.05.012>
59. Hou X, Roos P (2008) Critical comparison of radiometric and mass spectrometric methods for the determination of radionuclides in environmental, biological and nuclear waste samples. *Anal Chim Acta* 608:105–139. <https://doi.org/10.1016/j.aca.2007.12.012>
60. Morss LR, Edelstein NM, Fuger J (2006) The chemistry of the actinide and transactinide elements, 3rd edn. Springer, Dordrecht, pp 1–5
61. Boulyga SF, Testa C, Desideri D, Becker JS (2001) Optimisation and application of ICP-MS and alpha-spectrometry for determination of isotopic ratios of depleted uranium and plutonium in samples collected in Kosovo. *J Anal Atom Spectrom* 16:1283–1289. <https://doi.org/10.1039/B103178N>
62. Corcho Alvarado JA, Nedjadi Y, Bochud F (2011) Determining the activity of  $^{241}\text{Pu}$  by liquid scintillation counting. *J Radioanal Nucl Chem* 289:375–379. <https://doi.org/10.1007/s10967-011-1105-z>
63. McAninch JE, Hamilton TF, Brown TA, Jokela TA, Knezovich JP, Ognibene TJ, Proctor ID, Roberts ML, Sideras-Haddad E, Southon JR, Vogel JS (2000) Plutonium measurements by accelerator mass spectrometry at LLNL. *Nucl Instrum Methods*

- Phys Res B Beam Interact Mater Atom 172:711–716. [https://doi.org/10.1016/S0168-583X\(00\)00091-4](https://doi.org/10.1016/S0168-583X(00)00091-4)
64. Fifield LK, Cresswell RG, Tada ML, Ophel TR, Day JP, Clacher AP, King SJ, Priest ND (1996) Accelerator mass spectrometry of plutonium isotopes. *Nucl Instrum Methods Phys Res B Beam Interact Mater Atom* 117:295–303. [https://doi.org/10.1016/0168-583X\(96\)00287-X](https://doi.org/10.1016/0168-583X(96)00287-X)
  65. López-Lora M, Chamizo E, Villa-Alfageme M, Hurtado-Bermúdez S, Casacuberta N, García-León M (2018) Isolation of <sup>236</sup>U and <sup>239,240</sup>Pu from seawater samples and its determination by accelerator mass spectrometry. *Talanta* 178:202–210. <https://doi.org/10.1016/j.talanta.2017.09.026>
  66. López-Lora M, Levy I, Chamizo E (2019) Simple and fast method for the analysis of <sup>236</sup>U, <sup>237</sup>Np, <sup>239</sup>Pu and <sup>240</sup>Pu from seawater samples by accelerator mass spectrometry. *Talanta* 200:22–30. <https://doi.org/10.1016/j.talanta.2019.03.036>
  67. Thakur P (2019) Radiochemical methods I food and environmental applications. *Encyclopedia of analytical science*. Academic Press, London, pp 1–14
  68. Ketterer ME, Szechenyi SC (2008) Determination of plutonium and other transuranic elements by inductively coupled plasma mass spectrometry: a historical perspective and new frontiers in the environmental sciences. *Spectrochim Acta B Atom Spectrosc* 63:719–737. <https://doi.org/10.1016/j.sab.2008.04.018>
  69. Muramatsu Y, Hamilton T, Uchida S, Tagami K, Yoshida S, Robison W (2001) Measurement of <sup>240</sup>Pu/<sup>239</sup>Pu isotopic ratios in soils from the Marshall Islands using ICP-MS. *Sci Total Environ* 278:151–159. [https://doi.org/10.1016/S0048-9697\(01\)00644-1](https://doi.org/10.1016/S0048-9697(01)00644-1)
  70. Bu W, Gu M, Ding X, Ni Y, Shao X, Liu X, Yang C, Hu S (2021) Exploring the ability of triple quadrupole inductively coupled plasma mass spectrometry for the determination of Pu isotopes in environmental samples. *J Anal Atom Spectrom* 36:2330–2337. <https://doi.org/10.1039/D1JA00288K>
  71. Zheng J, Yamada M (2005) Vertical distributions of <sup>239</sup>+<sup>240</sup>Pu activities and <sup>240</sup>Pu/<sup>239</sup>Pu atom ratios in sediment cores: implications for the sources of Pu in the Japan Sea. *J Radioanal Nucl Chem* 340:199–211. <https://doi.org/10.1007/s10967-006-7001-2>
  72. Olufson KP, Moran G (2016) Polyatomic interference removal using a collision reaction interface for plutonium determination in the femtogram range by quadrupole ICP-MS. *J Radioanal Nucl Chem* 308:639–647. <https://doi.org/10.1007/s10967-015-4483-9>
  73. Zhang W, Lin J, Fang S, Li C, Yi X, Hou X, Chen N, Zhang H, Xu Y, Dang H, Wang W, Xu J (2021) Determination of ultra-trace level plutonium isotopes in soil samples by triple-quadrupole inductively coupled plasma-mass spectrometry with mass-shift mode combined with UTEVA chromatographic separation. *Talanta* 234:122652. <https://doi.org/10.1016/j.talanta.2021.122652>
  74. Vais V, Li C, Cornett J (2004) Separation of plutonium from uranium using reactive chemistry in a bandpass reaction cell of an inductively coupled plasma mass spectrometer. *Anal Bioanal Chem* 380:235–239. <https://doi.org/10.1007/s00216-004-2673-3>
  75. Tanner SD, Li C, Vais V, Baranov VI, Bandura DR (2004) Chemical resolution of Pu<sup>+</sup> from U<sup>+</sup> and Am<sup>+</sup> using a band-pass reaction cell inductively coupled plasma mass spectrometer. *Anal Chem* 76:3042–3048. <https://doi.org/10.1021/ac049899j>
  76. Gourgiotis A, Granet M, Isnard H, Nonell A, Gautier C, Stadelmann G, Aubert M, Durand D, Legand S, Chartier F (2010) Simultaneous uranium/plutonium separation and direct isotope ratio measurements by using CO<sub>2</sub> as the gas in a collision/reaction cell based MC-ICPMS. *J Anal Atom Spectrom* 25:1939–1945. <https://doi.org/10.1039/C0JA00092B>
  77. Childs DA, Hill JG (2018) The use of carbon dioxide as the reaction cell gas for the separation of uranium and plutonium in quadrupole inductively coupled plasma mass spectrometry (ICP-MS) for nuclear forensic samples. *J Radioanal Nucl Chem* 318:139–148. <https://doi.org/10.1007/s10967-018-5973-3>
  78. Amr MA, Helal AFI, Al-Kinani AT, Balakrishnan P (2016) Ultra-trace determination of <sup>90</sup>Sr, <sup>137</sup>Cs, <sup>238</sup>Pu, <sup>239</sup>Pu, and <sup>240</sup>Pu by triple quadrupole collision/reaction cell-ICP-MS/MS: establishing a baseline for global fallout in Qatar soil and sediments. *J Environ Radioact* 153:73–87. <https://doi.org/10.1016/j.jenvrad.2015.12.008>
  79. Xu Y, Li C, Yu H, Fang F, Hou X, Zhang C, Xiaofei Li, Xing S (2022) Rapid determination of plutonium isotopes in small samples using single anion exchange separation and ICP-MS/MS measurement in NH<sub>3</sub>-He mode for sediment dating. *Talanta* 240:123152. <https://doi.org/10.1016/j.talanta.2021.123152>
  80. Tiong LYD, Tan S (2019) In situ determination of <sup>238</sup>Pu in the presence of uranium by triple quadrupole ICP-MS (ICP-QQQ-MS). *J Radioanal Nucl Chem* 322:399–406. <https://doi.org/10.1007/s10967-019-06695-3>
  81. Moldovan M, Krupp EM, Holliday AE, Donard OFX (2004) High resolution sector field ICP-MS and multicollector ICP-MS as tools for trace metal speciation in environmental studies: a review. *J Anal Atom Spectrom* 19:815–822. <https://doi.org/10.1039/B403128H>
  82. Jakubowski N, Moens L, Vanhaecke F (1998) Sector field mass spectrometers in ICP-MS. *Spectrochim Acta B Atom Spectrosc* 53:1739–1763. [https://doi.org/10.1016/S0584-8547\(98\)00222-5](https://doi.org/10.1016/S0584-8547(98)00222-5)
  83. Donard OFX, Bruneau F, Moldovan M, Garraud H, Epov VN, Boust D (2007) Multi-isotopic determination of plutonium (<sup>239</sup>Pu, <sup>240</sup>Pu, <sup>241</sup>Pu and <sup>242</sup>Pu) in marine sediments using sector-field inductively coupled plasma mass spectrometry. *Anal Chim Acta* 587:170–179. <https://doi.org/10.1016/j.aca.2007.01.047>
  84. Zheng J, Yamada M (2006) Inductively coupled plasma-sector field mass spectrometry with a high-efficiency sample introduction system for the determination of Pu isotopes in settling particles at femtogram levels. *Talanta* 69:1246–1253. <https://doi.org/10.1016/j.talanta.2005.12.047>
  85. Pointurier F, Pottin AC, Hémet P, Hubert A (2011) Combined use of medium mass resolution and desolvation introduction system for accurate plutonium determination in the femtogram range by inductively coupled plasma-sector-field mass spectrometry. *Spectrochim Acta B Atom Spectrosc* 66:261–267. <https://doi.org/10.1016/j.sab.2011.03.003>
  86. Liao H, Zheng J, Wu F, Yamada M, Tan M, Chen J (2008) Determination of plutonium isotopes in freshwater lake sediments by sector-field ICP-MS after separation using ion-exchange chromatography. *Appl Radiat Isotope* 66:1138–1145. <https://doi.org/10.1016/j.apradiso.2008.01.001>
  87. Guan Y, Sun S, Sun S, Wang H, Ruan X, Liu Z, Terrasi F, Gialanella L, Shen H (2018) Distribution and sources of plutonium along the coast of Guangxi, China. *Nucl Instrum Methods Phys Res B Beam Interact Mater Atom* 437:61–65. <https://doi.org/10.1016/j.nimb.2018.09.047>
  88. Huang Z, Ni Y, Wang H, Zheng J, Yamazaki S, Sakaguchi A, Long X, Uchida S (2019) Simultaneous determination of ultra-trace level <sup>237</sup>Np and Pu isotopes in soil and sediment samples by SF-ICP-MS with a single column chromatographic separation. *Microchem J* 148:597–604. <https://doi.org/10.1016/j.micro.2019.05.044>
  89. Taylor RN, Warneke T, Milton JA, Croudace IW, Warwick PE, Nesbitt RW (2003) Multiple ion counting determination of plutonium isotope ratios using multi-collector ICP-MS. *J Anal Atom Spectrom* 18:480–484. <https://doi.org/10.1039/B300432E>
  90. Lindahl P, Keith-Roach M, Worsfold P, Choi MS, Shin HS, Lee SH (2010) Ultra-trace determination of plutonium in marine

- samples using multi-collector inductively coupled plasma mass spectrometry. *Anal Chim Acta* 671:61–69. <https://doi.org/10.1016/j.aca.2010.05.012>
91. Taylor RN, Warneke T, Milton JA, Croudace IW, Warwick PE, Nesbitt RW (2001) Plutonium isotope ratio analysis at femtogram to nanogram levels by multicollector ICP-MS. *J Anal Atom Spectrom* 16:279–284. <https://doi.org/10.1039/B009078F>
92. Ronzani AL, Pointurier F, Rittner M, Borovinskaya TM, Hubert A, Humbert AC, Aupiais J, Dacheux N (2018) Capabilities of laser ablation—ICP-TOF-MS coupling for isotopic analysis of individual uranium micrometric particles. *J Anal Atom Spectrom* 33:1892–1902. <https://doi.org/10.1039/C8JA00241J>
93. Cizdziel JV (2007) Determination of lead in blood by laser ablation ICP-TOF-MS analysis of blood spotted and dried on filter paper: a feasibility study. *Anal Bioanal Chem* 388:603–611. <https://doi.org/10.1007/s00216-007-1242-y>
94. Baalousha M, Wang J, Erfani M, Goharian E (2021) Elemental fingerprints in natural nanomaterials determined using SP-ICP-TOF-MS and clustering analysis. *Sci Total Environ* 792:148426. <https://doi.org/10.1016/j.scitotenv.2021.148426>
95. Greenhalgh CJ, Voloaca OM, Shaw P, Donard A, Cole LM, Clench MR, Managh AJ, Haywood-small SL (2020) Needles in haystacks: using fast-response LA chambers and ICP-TOF-MS to identify asbestos fibres in malignant mesothelioma models. *J Anal Atom Spectrom* 35:2231–2238. <https://doi.org/10.1039/D0JA00268B>
96. Bauer OB, Hachmoller O, Borovinskaya O, Sperling M, Schurek HJ, Ciarimboli G, Karst U (2019) LA-ICP-TOF-MS for rapid, all-elemental and quantitative bioimaging, isotopic analysis and the investigation of plasma processes. *J Anal Atom Spectrom* 34:694–701. <https://doi.org/10.1039/C8JA00288F>
97. Saha A, Deb SB, Saxena MK (2016) Determination of trace impurities in advanced metallic nuclear fuels by inductively coupled plasma time-of-flight mass spectrometry (ICP-TOF-MS). *J Anal Atom Spectrom* 31:1480–1489. <https://doi.org/10.1039/C6JA00138F>
98. Kazi ZH, Cornett JR, Zhao X, Kieser L (2014) Americium and plutonium separation by extraction chromatography for determination by accelerator mass spectrometry. *Anal Chim Acta* 829:75–80. <https://doi.org/10.1016/j.aca.2014.04.044>
99. Wang ZT, Zheng J, Imanaka T, Uchida S (2017) A rapid method for accurate determination of  $^{241}\text{Am}$  by sector field inductively coupled plasma mass spectrometry and its application to Sellafield site soil samples. *J Anal Atom Spectrom* 32:2034–2040. <https://doi.org/10.1039/C7JA00201G>
100. Shin C, Choi H, Kwon H, Jo H, Kim H, Yoon H, Kim D, Kang G (2017) Determination of plutonium isotopes ( $^{238}\text{Pu}$ ,  $^{239}\text{Pu}$ ,  $^{240}\text{Pu}$ ) and strontium ( $^{90}\text{Sr}$ ) in seafood using alpha spectrometry and liquid scintillation spectrometry. *J Environ Radioact* 177:151–157. <https://doi.org/10.1016/j.jenvrad.2017.06.025>
101. Mhatre AM, Chappa S, Paul S, Pandey AK (2017) Phosphate-bearing polymer grafted glass for plutonium(IV) ion-selective alpha spectrometry. *J Anal Atom Spectrom* 32:1566–1570. <https://doi.org/10.1039/C7JA00156H>
102. Seferinoğlu M, Aslan N, Kurt A, Erden PE, Mert H (2014) Determination of plutonium isotopes in bilberry using liquid scintillation spectrometry and alpha-particle spectrometry. *Appl Radiat Isotope* 87:81–86. <https://doi.org/10.1016/j.apradiso.2013.11.097>
103. Liu B, Shi K, Ye G, Guo Z, Wu W (2016) Method development for plutonium analysis in environmental water samples using TEVA microextraction chromatography separation and low background liquid scintillation counter measurement. *Microchem J* 124:824–830. <https://doi.org/10.1016/j.microc.2015.10.007>
104. Yamamoto M, Taguchi S, Do VK, Kuno T, Surugaya N (2019) Development of an online measurement system using an alpha liquid scintillation counter and a glass-based microfluidic solvent extraction device for plutonium analysis. *Appl Radiat Isotope* 152:37–44. <https://doi.org/10.1016/j.apradiso.2019.06.027>
105. Dai X, Christl M, Kramer-Tremblay S, Synal HA (2012) Ultra-trace determination of plutonium in urine samples using a compact accelerator mass spectrometry system operating at 300 kV. *J Anal Atom Spectrom* 27:126–130. <https://doi.org/10.1039/C1JA10264H>
106. Strumińska-Parulska DI (2013) Accelerator mass spectrometry (AMS) in plutonium analysis. *J Radioanal Nucl Chem* 298:593–598. <https://doi.org/10.1007/s10967-013-2448-4>
107. Kaplan DI, Demirkanli DI, Molz FJ, Beals DM, Cadieux JR, Halverson JE (2010) Upward movement of plutonium to surface sediments during an 11-year field study. *J Environ Radioact* 101:338–344. <https://doi.org/10.1016/j.jenvrad.2010.01.007>
108. Lee CG, Suzuki D, Esaka F, Magara M, Song K (2015) Ultra-trace analysis of plutonium by thermal ionization mass spectrometry with a continuous heating technique without chemical separation. *Talanta* 141:92–96. <https://doi.org/10.1016/j.talanta.2015.03.060>
109. Epov VN, Benkhedda K, Cornett RJ, Evans RD (2005) Rapid determination of plutonium in urine using flow injection on-line preconcentration and inductively coupled plasma mass spectrometry. *J Anal Atom Spectrom* 20:424–430. <https://doi.org/10.1039/B501218J>
110. Epov VN, Benkhedda K, Evans RD (2005) Determination of Pu isotopes in vegetation using a new on-line FI-ICP-DRC-MS protocol after microwave digestion. *J Anal Atom Spectrom* 20:990–992. <https://doi.org/10.1039/B504569J>
111. Truscott JB, Jones P, Fairman BE, Evans EH (2001) Determination of actinide elements at femtogram per gram levels in environmental samples by on-line solid phase extraction and sector-field-inductively coupled plasma-mass spectrometry. *Anal Chim Acta* 433:245–253. [https://doi.org/10.1016/S0003-2670\(01\)00784-X](https://doi.org/10.1016/S0003-2670(01)00784-X)
112. Mitroshkov AV, Olsen KB, Thomas ML (2015) Estimation of the formation rates of polyatomic species of heavy metals in plutonium analyses using a multicollector ICP-MS with a desolvating nebulizer. *J Anal Atom Spectrom* 30:487–493. <https://doi.org/10.1039/C4JA00282B>